In Situ Transmission Electron Microscopy Study of Molybdenum Oxide Contacts for Silicon Solar Cells

Haider Ali, Supriya Koul, Geoffrey Gregory, James Bullock, Ali Javey, Akihiro Kushima, and Kristopher O. Davis*

In this study, a molybdenum oxide (MoO$_x$) and aluminum (Al) contact structure for crystalline silicon (c-Si) solar cells is investigated using a combination of transmission line measurements (TLM) and in-situ transmission electron microscopy (TEM). Cross-sectional high-resolution TEM (HRTEM) micrographs reveal a $\approx$2 nm silicon oxide (SiO$_x$) interlayer at c-Si/MoO$_x$ interface in the as-deposited state, indicating that formation of SiO$_x$ occurs during deposition of MoO$_x$. Moreover, oxygen diffusion takes place from MoO$_x$ toward Al resulting in the formation of a $\approx$2–3 nm aluminum oxide (AlO$_x$) interlayer at the MoO$_x$/Al interface. Overall, it is observed that MoO$_x$/Al contact is relatively stable upon annealing up to 200 °C and still retains ohmic transport with sufficiently low contact resistivity.

1. Introduction

To minimize recombination losses in crystalline silicon solar cells, it is essential to obtain low recombination velocities both in the bulk as well as at the Si surface. Bulk recombination is taken care of by using a high-quality Si wafer. To minimize surface recombination, it is essential to have excellent surface passivation as well as suitable carrier-selectivity at both front and rear contacts. This can be accomplished with carrier selective contacts at both front and rear contact regions. For instance, doped hydrogenated amorphous silicon (a-Si:H) in combination with an ultra-thin a-Si:H(i) or SiO$_2$ are often employed as carrier selective contacts in silicon heterojunction (SHJ) solar cells. In such cases, a-Si:H(n) and a-Si:H(p) act as electron-selective and hole-selective contacts respectively. The role of a-Si:H(i) is to act

Dr. H. Ali, S. Koul, G. Gregory, Dr. A. Kushima, K. O. Davis
Department of Materials Science and Engineering
University of Central Florida
Orlando, FL, USA
E-mail: kristopher.davis@ucf.edu

H. Ali, G. Gregory, Dr. K. O. Davis
Florida Solar Energy Center
University of Central Florida
Cocoa, FL, USA

Dr. J. Bullock, Prof. A. Javey
Department of Electrical Engineering and Computer Science
University of California
Berkeley, CA, USA

The ORCID identification number(s) for the author(s) of this article can be found under https://doi.org/10.1002/pssa.201800998.

DOI: 10.1002/pssa.201800998

as buffer layer apart from passivating the Si surface whereas SiO$_2$ solely acts as a passivation layer.[1–9]

Recently, transition metal oxides have emerged as promising materials to be employed as Carrier selective contacts in SHJ cells. Typically, they consist of a thin (<10 nm) transition metal oxide layer used in combination with a-Si:H(i) or SiO$_2$ at front and rear contact regions of Si solar cells. In some cases, the carrier-selectivity of these contacts is dependent on the valence-band and conduction-band offset between the metal oxide and Si. For instance, titanium oxide (TiO$_2$) behaves as an electron-selective contact because the small conduction band offset ($\Delta E_c = 0.05$ eV) with Si allows electrons to pass through the TiO$_2$ layer and the large valence-band offset ($\Delta E_v = 2.0$ eV) leads to hole blocking. Cell efficiencies up to 21.6% have been reported for n-type cells featuring SiO$_2$/TiO$_2$/Al rear contact.[6,7,10,11]

Likewise, wide band gap and high work function substochiometric metal oxides such as molybdenum oxide (MoO$_x$), tungsten oxide (WO$_x$), and vanadium oxide (VO$_x$) have emerged as effective hole-selective contacts in Si solar cells. The large work function difference between Si and these n-type metal oxides induces a strong upward band bending in Si, lowering the electron concentration at the surface. The wide band gap (>3 eV) of these materials results in high transparency, and they have therefore been used as hole-selective front contacts in combination with transparent conducting oxide (TCO) window layers such as hydrogenated indium oxide (IO:H) or indium tin oxide (ITO).[2,12–16] However, a major limitation of these contact structures is that they are sensitive to low temperature annealing resulting in degradation of device performance. Although, the origin of these losses is yet to be fully understood, it appears that the poor performance is due to a reduction in the work function upon annealing and resulting loss of hole-selectivity.[17,18]

Carrier selective contacts can also be formed using transition metal oxides in direct contact with metal such as Al. For instance, WO$_x$/Al has been investigated as potential hole-selective rear contact for a p-type c-Si solar cell.[19] It was further revealed that although WO$_x$/Al is stable up to 400 °C, it exhibits non-ohmic behavior.[20] In the present work, WO$_x$/Al was replaced by MoO$_x$/Al in order to obtain ohmic transport with low contact resistivity when subjected to low temperature annealing. For this purpose, the thermal stability of c-Si/MoO$_x$/Al contact structure was investigated with the help of in-situ transmission electron

microscopy (TEM). Furthermore, the contact resistivity at various annealing temperatures was measured by transmission line measurements (TLM).

2. Experimental Section

MoO_x thin films (<10 nm) were deposited on p-type FZ (100) c-Si wafers under vacuum by thermal evaporation wherein a powder MoO_3 source was used. During the evaporation process, Si substrate remained at ambient temperature. Finally, 500 nm of Al was evaporated over MoO_x. A schematic of test structure used for TLM measurement is shown as an inset in **Figure 1**.

Dark current-voltage (I–V) curves were measured for several contact pairs at different spacings at various annealing temperatures using a Kiethley 2400 Sourcemeter. This data was then used to extract the contact resistivity of the MoO_x/Al contact stack. To account for current spreading occurring due to absence of an emitter, the extended TLM was used.[21]

For TEM studies, cross-sectional TEM specimen was prepared by focused ion beam (FIB) milling technique using FEI 200 TEM FIB. The in-situ TEM experiments were performed with the help of FEI Tecnai F30 under operating voltage of 300 KV. Cross-sectional TEM specimen was heated in-situ using Gatan heating holder (Model 652) up to temperature of 400 °C at a heating rate of 50 °C min^{-1}. with annealing time of 10 min.

3. Results and Discussion

The contact resistivity values obtained at various annealing temperatures by TLM are shown in Figure 1. It is evident that MoO_x/Al exhibits ohmic character in the as-deposited state with a low contact resistivity value of 24 mΩ · cm^2. On the other hand, cross-sectional HRTEM images revealed that 2–3 nm SiO_x
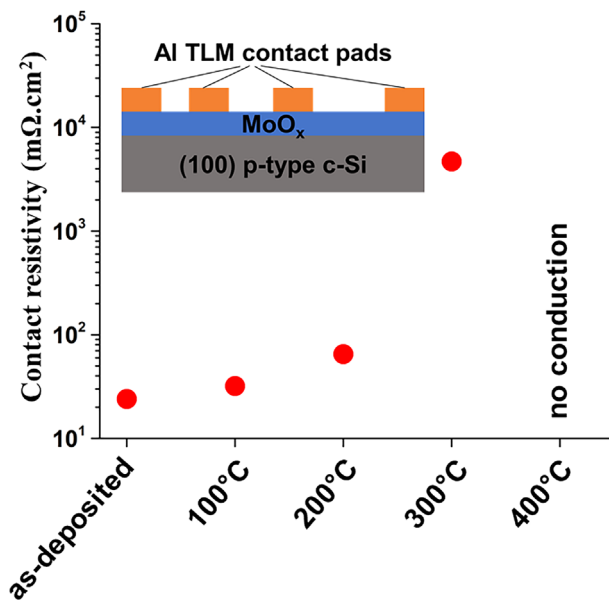

Figure 1. Contact resistivity at various annealing temperatures obtained by TLM.

interlayer is present at c-Si/MoO_x interface even in the as-deposited state (**Figure 2**a). This indicates that SiO_x interlayer was formed during thermal evaporation of MoO_x over Si substrate. This is consistent with observations reported by Gerling et al.[15] It has been previously reported that the SiO_x interlayer is sub-stochiometric and therefore allows conduction of charge carriers through it.[15,16] The net effect is that the conduction of charge carriers in the MoO_x/Al contact is not adversely affected by the presence of sub-stochiometric SiO_x interlayer.

Moreover, MoO_x/Al retains its hole-blocking ability even in presence of SiO_x which is evident from the simulated band diagram of c-Si/SiO_x/MoO_x/Al contact structure as shown in Figure 3. This was obtained with the help of wxAMPS.[22]

Furthermore, HRTEM images further revealed the presence of an AlO_x interlayer at the MoO_x/Al interface in the as-deposited state (Figure 2a). This can be attributed to favorable thermodynamic conditions.[23] The higher oxygen affinity of Al compared to Mo is the driving force for oxygen diffusion from MoO_x toward Al resulting in the formation of AlO_x interlayer as well as creation of defect states within MoO_x layer.

When the annealing temperature is increased to 200 °C, AlO_x and MoO_x layers are clearly distinguishable which indicates that no major change occurs at MoO_x/AlO_x interface. However, SiO_x layers become diffused and less obvious at 200 °C (Figure 2b and video 2b, Supporting Information). Overall, it can be inferred that c-Si/MoO_x/Al contact structure is relatively stable with no significant changes occurring up to 200 °C. This is further supported by TLM measurements which revealed that MoO_x/Al retains its ohmic behavior when annealed to 100 °C and subsequently to 200 °C. Further, low contact resistivity values of 32 and 65 mΩ · cm^2 are obtained at 100 and 200 °C, respectively.

When annealing temperature is further increased to 300 °C, significant intermixing appears to take place and the AlO_x interlayer becomes indistinguishable from the Al contact, but the MoO_x layer still appears to be intact (Figure 2c and video 2c, Supporting Information). This can be attributed to enhanced surface diffusion at the nano-scale which enables intermixing at relatively lower temperatures. More importantly, a drastic increase in contact resistivity occurs at 300 °C which is demonstrated by the high contact resistivity value of 4700 mΩ · cm^2. Interestingly, the MoO_x/Al contact structure still retains ohmic transport.

Subsequently, at 400 °C, intermixing appears to be complete which results in MoO_x/Al contact structure becoming non-ohmic and no conduction is observed during TLM measurements (Figure 2d and video 2d, Supporting Information).

Overall, the MoO_x/Al contact exhibits ohmic behavior and sufficiently low contact resistivity values up to 200 °C. This is in marked contrast to a-Si:H(i)/MoO_x/ITO contact structure wherein a drastic increase in contact resistivity is observed upon annealing up to 200 °C.[17,18]

In a nutshell, MoO_x/Al can withstand low temperature anneals and still exhibit ohmic behavior with sufficiently low contact resistivity values (65 mΩ · cm^2). The low contact resistivity of MoO_x/Al up to 200 °C is a significant improvement compared to WO_x/Al which exhibits non-ohmic behavior even up to 400 °C.[20]
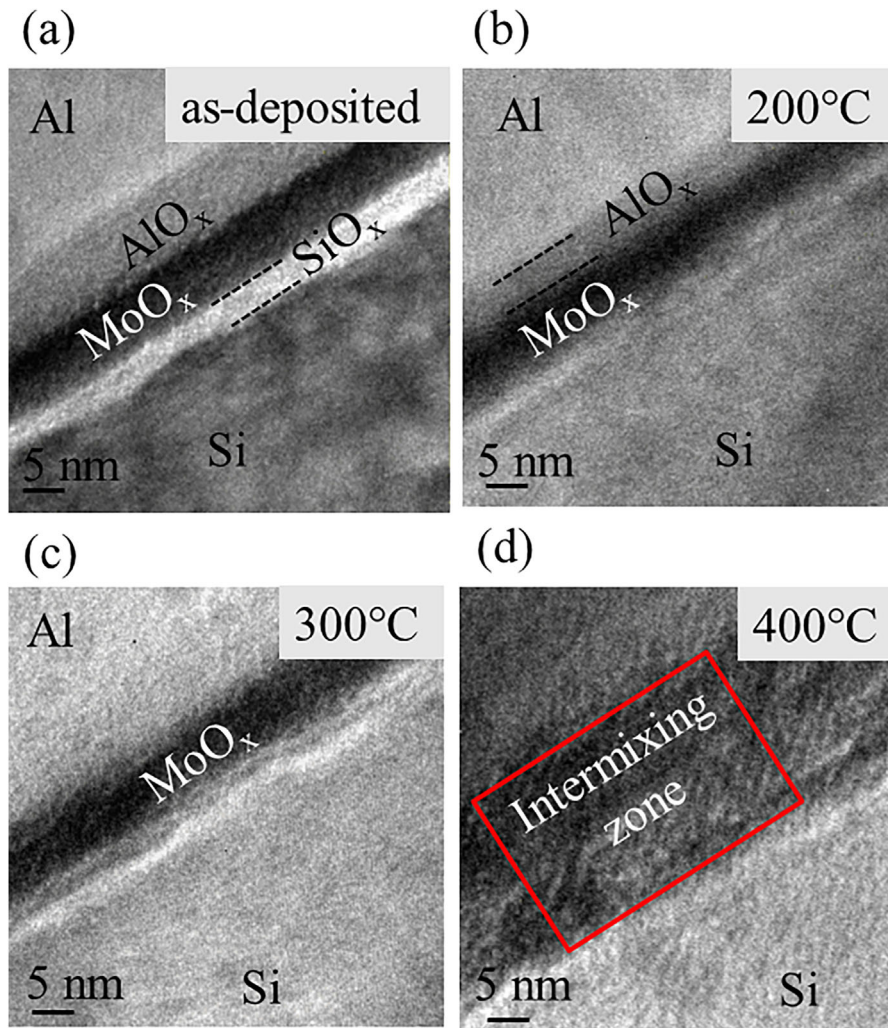
Figure 2. Cross-sectional HRTEM micrograph of c-Si/MoO$_x$/Al structure obtained by in-situ TEM studies: (a) as-deposited (b) 200 °C (c) 300 °C (d) 400 °C.
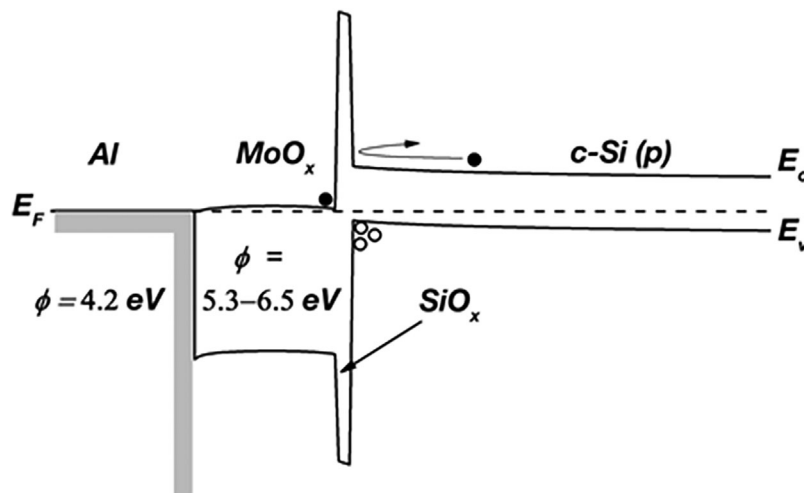

Figure 3. The energy band diagram of the MoO$_x$/Al contact to p-type c-Si with 2 nm of SiO$_x$.

**ADVANCED
SCIENCE NEWS**

www.advancedsciencenews.com

pss
physica status solidi a

www.pss-a.com

4. Conclusion

In summary, MoO_x/Al contact structures have the ability to withstand annealing temperatures up to 200 °C without any significant degradation and still retain ohmic character with sufficiently low contact resistivity. Therefore, MoO_x/Al can be a potential candidate to be employed as a hole-selective rear contact for a *p*-type c-Si solar cell. Moreover, it has been demonstrated that in-situ TEM studies can be used to obtain valuable information about the thermal stability of contact structures formed by various combinations of transition metal oxides and metal contacts employed in high efficiency c-Si solar cells.

Supporting Information

Supporting Information is available from the Wiley Online Library or from the author.

Conflict of Interest

The authors declare no conflict of interest.

[1] H. Ali, X. Yang, K. Weber, W. V. Schoenfeld, K. O. Davis, *Microsc. Microanal.* **2017**, *23*, 900.

[2] M. Bivour, J. Temmler, H. Steinkemper, M. Hermle, *Sol. Energy Mater. Sol. Cells* **2015**, *142*, 34.

[3] F. Feldmann, M. Simon, M. Bivour, C. Reichel, M. Hermle, S. W. Glunz, *Appl. Phys. Lett.* **2014**, *104*, 181105.

[4] A. G. Aberle, *Prog. Photovoltaics Res. Appl.* **2000**, *8*, 473.

[5] A. G. Aberle, *Sol. Energy Mater. Sol. Cells* **2001**, *65*, 239.

[6] X. Yang, Q. Bi, H. Ali, K. Davis, W. V. Schoenfeld, K. Weber, *Adv. Mater.* **2016**, *28*, 5891.

[7] X. Yang, P. Zheng, Q. Bi, K. Weber, *Sol. Energy Mater. Sol. Cells* **2016**, *150*, 32.

[8] J. Bullock, A. Cuevas, C. Samundsett, D. Yan, J. McKeon, Y. Wan, *Sol. Energy Mater. Sol. Cells* **2015**, *138*, 22.

[9] J. Bullock, D. Yan, Y. Wan, A. Cuevas, B. Demaurex, A. Hessler-Wyser, S. De Wolf, *J. Appl. Phys.* **2014**, *115*, 163703.

[10] X. Yang, K. Weber, N-type silicon solar cells featuring an electron-selective TiO_2 contact, Photovoltaic Specialist Conference (PVSC), 2015 IEEE 42nd, **2015**, pp. 1–4.

[11] T. G. Allen, J. Bullock, Q. Jeangros, C. Samundsett, Y. Wan, J. Cui, A. Hessler-Wyser, S. De Wolf, A. Javey, A. Cuevas, *Adv. Energy Mater.* **2017**, *7*, 1602606-n/a.

[12] C. Battaglia, X. Yin, M. Zheng, I. D. Sharp, T. Chen, S. McDonnell, A. Azcatl, C. Carraro, B. Ma, R. Maboudian, R. M. Wallace, A. Javey, *Nano Lett.* **2014**, *14*, 967.

[13] M. Bivour, B. Macco, J. Temmler, W. M. M. Kessels, M. Hermle, *Energy Procedia* **2016**, *92*, 443.

[14] L. G. Gerling, S. Mahato, A. Morales-Vilches, G. Masmitja, P. Ortega, C. Voz, R. Alcubilla, J. Puigdollers, *Sol. Energy Mater. Sol. Cells* **2016**, *145*, 109.

[15] L. G. Gerling, C. Voz, R. Alcubilla, J. Puigdollers, *J. Mater. Res.* **2016**, *32*, 260.

[16] D. Sacchetto, Q. Jeangros, G. Christmann, L. Barraud, A. Descoeudres, J. Geissbühler, M. Despeisse, A. Hessler-Wyser, S. Nicolay, C. Ballif, *IEEE J. Photovoltaics* **2017**, *7*, 1584.

[17] J. Geissbühler, J. Werner, S. M. d. Nicolas, L. Barraud, A. Hessler-Wyser, M. Despeisse, S. Nicolay, A. Tomasi, B. Niesen, S. D. Wolf, C. Ballif, *Appl. Phys. Lett.* **2015**, *107*, 081601.

[18] L. Neusel, M. Bivour, M. Hermle, *Energy Procedia* **2017**, *124*, 425.

[19] C.-Y. Lee, M. I. A. Aziz, S. Wenham, B. Hoex, *Jpn. J. Appl. Phys.* **2017**, *56*, 08MA08.

[20] H. Ali, S. Koul, G. Gregory, J. Bullock, A. Javey, A. Kushima, K. O. Davis, *Sci. Rep.* **2018**, *8*, 12651.

[21] E. G. Woelk, H. Krautle, H. Beneking, *IEEE Trans. Electron Devices* **1986**, *33*, 19.

[22] Y. Liu, D. Heinzel, A. Rockett, A new solar cell simulator: WxAMPS, 2011 37th IEEE Photovoltaic Specialists Conference, 2011, pp. 002753–002756.

[23] H.-Y. Zhu, R. Gao, W.-T. Jin, L.-W. Qiu, Z.-L. Xue, *Rare Met.* **2018**, *37*, 621.